J Arid Land (2021) 13(5): 455–469
https://doi.org/10.1007/s40333-021-0100-7

Science Press Springer-Verlag

Quantification of groundwater recharge and evapotranspiration along a semi-arid wetland transect using diurnal water table fluctuations

JIA Wuhui[1], YIN Lihe[2*], ZHANG Maosheng[3], ZHANG Xinxin[4], ZHANG Jun[2], TANG Xiaoping[2], DONG Jiaqiu[2]

[1] School of Water Resources and Environment, China University of Geosciences (Beijing), Beijing 100083, China;
[2] Xi'an Center of Geological Survey, China Geological Survey, Xi'an 710054, China;
[3] Institute of Disaster Prevention and Ecological Restoration, Xi'an Jiaotong University, Xi'an 710049, China;
[4] Chinese Academy of Geological Sciences, Beijing 100037, China

Abstract: Groundwater is a vital water resource in arid and semi-arid areas. Diurnal groundwater table fluctuations are widely used to quantify rainfall recharge and groundwater evapotranspiration (ET_g). To assess groundwater resources for sustainable use, we estimated groundwater recharge and ET_g using the diurnal water table fluctuations at three sites along a section with different depths to water table (DWT) within a wetland of the Mukai Lake in the Ordos Plateau, Northwest China. The water table level was monitored at an hourly resolution using a Keller DCX-22A data logger that measured both the total pressure and barometric pressure, so that the effect of barometric pressure could be removed. At this study site, a rapid water table response to rainfall was observed in two shallow wells (i.e., Obs1 and Obs2), at which diurnal water table fluctuations were also observed over the study period during rainless days, indicating that the main factors influencing water table variation are rainfall and ET_g. However, at the deep-water table site (Obs3), the groundwater level only reacted to the heaviest rainfalls and showed no diurnal variations. Groundwater recharge and ET_g were quantified for the entire hydrological year (June 2017–June 2018) using the water table fluctuation method and the Loheide method, respectively, with depth-dependent specific yields. The results show that the total annual groundwater recharge was approximately 207 mm, accounting for 52% of rainfall at Obs1, while groundwater recharge was approximately 250 and 21 mm at Obs2 and Obs3, accounting for 63% and 5% of rainfall, respectively. In addition, the rates of groundwater recharge were mainly determined by rainfall intensity and DWT. The daily mean ET_g at Obs1 and Obs2 over the study period was 4.3 and 2.5 mm, respectively, and the main determining factors were DWT and net radiation.

Keywords: groundwater recharge; groundwater evapotranspiration; water table fluctuation; semi-arid region; Ordos Plateau

Citation: JIA Wuhui, YIN Lihe, ZHANG Maosheng, ZHANG Xinxin, ZHANG Jun, TANG Xiaoping, DONG Jiaqiu. 2021. Quantification of groundwater recharge and evapotranspiration along a semi-arid wetland transect using diurnal water table fluctuations. Journal of Arid Land, 13(5): 455–469. https://doi.org/10.1007/s40333-021-0100-7

1 Introduction

In (semi-) arid regions, groundwater plays a significant role in meeting urban, industrial, and

*Corresponding author: YIN Lihe (E-mail: ylihe@cgs.cn)
Received 2020-03-18; revised 2021-03-19; accepted 2021-04-08
© Xinjiang Institute of Ecology and Geography, Chinese Academy of Sciences, Science Press and Springer-Verlag GmbH Germany, part of Springer Nature 2021

agricultural water requirements because of the unreliability or under-allocation of surface water. Globally, more than two billion people depend on groundwater, and approximately 50% of irrigation water is obtained from groundwater (Alley et al., 2002; Siebert et al., 2010). Due to unsustainable development practices, groundwater depletion has taken place in many regional aquifers worldwide, such as the North China Plain (Feng et al., 2013), the US High Plains (Scanlon et al., 2012), and the Nubian sandstone aquifer in North Africa (Doll et al., 2014).

Groundwater budget analysis is a critical component for the sustainable use of groundwater resources (Bredehoeft, 1997; Zhou, 2009) and the main components of groundwater budgets are rainfall recharge and groundwater evapotranspiration (ET_g) (Crosbie et al., 2005; Zhang et al., 2016). Many methods are available for estimating the infiltration recharge from rainfall and ET_g, including soil water balance (Allison et al., 1994; Gribovszki, 2018), water table fluctuations (WTFs) (Cheng et al., 2017; Delottier et al., 2018; Wang et al., 2019a) and numerical simulations (Loheide et al., 2005; Liu et al., 2014). Among these methods, the WTF (water table fluctuation) method is considered to be effective for quantifying rainfall recharge and ET_g because of its simplicity and ease of use (Healy and Cook, 2002). The application of WTF to estimate groundwater recharge can be traced back to the 1920s (Meinzer, 1923). The procedure used to estimate daily ET_g using diurnal WTFs was first developed by White (1932), but this method has only been widely used in recent decades because of the availability of automatic high-resolution groundwater data loggers that can detect millimeter-scale variations (Wang et al., 2019b; Gribovszki et al., 2010; Diouf et al., 2020). With recently applied modifications, the sub-daily ET_g can be estimated from diurnal WTFs (Gribovszki et al., 2008; Loheide, 2008; Yin et al., 2013).

Water tables in wetlands are shallow because of the convergence of surface runoff and lateral groundwater flows (Toth, 1962; Fan et al., 2013). Consequently, plant species are abundant around wetlands because of the high availability of water for their use (Busch et al., 1992; Sargeant and Singer, 2016). However, unsustainable groundwater use may degrade wetland ecosystems. For example, groundwater-dependent willows died after two years of groundwater pumping in a wetland in the USA (Scott et al., 2000).

The Ordos Plateau is located in Northwest China, where approximately 400 lake wetlands are present (Yin et al., 2011a). Natural resources are extremely abundant in the Ordos Plateau, including petroleum, natural gas, coal, and sandstone type uranium deposits (Chang et al., 2006). It contains the greatest natural gas reserves and the second greatest coal reserves in China (Dai et al., 2006). In recent years, groundwater from the area has been pumped out in increasing volumes to sustain the rapid development of the Ordos National Energy Base (Hou et al., 2008). The effects of overexploitation have already been observed in some areas, resulting in the drying up of artesian wells, degradation of groundwater quality, and dieback of groundwater-dependent ecosystems (Liu et al., 2015). This is due to the improper quantification of water budget components that adversely affect the sustainable development of groundwater resources and groundwater-dependent plants in lake wetlands (Liu et al., 2017). In previous studies on the groundwater budget in the Ordos Plateau (Wang et al., 2010; Liu et al., 2018), groundwater recharge was determined to be the product of annual rainfall and the coefficient of rainfall, without considering the impact of rainfall intensity, antecedent rainfall, and the depth to water table (DWT) on groundwater recharge. ET_g was calculated based on the linear relationship between the evapotranspiration (ET) flux at the surface and DWT. However, numerous studies indicate that this relationship is more complex than what can be effectively represented by a linear model (Baird and Maddock, 2005; Doble and Crosbie, 2017).

To improve water budget estimates, it is vital to quantify rainfall infiltration and groundwater evapotranspiration, as well as their main controlling factors. Therefore, hourly water table variations were monitored at three sites over a hydrological year in the semi-arid wetland around a lake in the Ordos Plateau. We estimated groundwater recharge and ET_g based on the monitoring data, and analyzed their controlling factors, such as DWT, rainfall intensity, and antecedent rainfall. The objectives of this study were to: (1) explore the response of the water table to rainfall and ET_g at different depths along a section; (2) estimate groundwater recharge and ET_g using a

depth-dependent specific yield; and (3) determine the hourly, daily, and monthly variations of rainfall infiltration and ET_g, as well as to quantify their controlling factors to explore the mechanisms affecting rainfall infiltration and ET_g at different time scales.

2 Materials and methods

2.1 Study site and experimental setup

The study site (39°17′26″N, 108°49′17″E) was located within the wetland of Mukai Lake in the Ordos Plateau, Northwest China (Fig. 1a). Geographically, it is located in the Middle East Ordos Plateau, where the climate is semi-arid and characterized by low rainfall and high ET_g. The study site was located within an area where groundwater recharges lakes (Yin et al., 2011a; Liu et al., 2015). The phreatophyte near the lake was native grasses, mainly *Carex stenophylla* and *Puccinellia tenuifolia*, with a root depth of approximately 80 cm. Although groundwater had not been extracted from this lake wetland, an adjacent lake wetland area was heavily pumped, and corresponding adverse environmental effects have been observed there, such as wetland shrinkage and ecosystem degradation (Liu et al., 2015, 2018). The local government is planning to reassess safe pumping rates and requires a detailed water budget analysis. Because of the similar hydrogeological and meteorological conditions, the results of this study can provide a reference for other lake wetlands in the Ordos Plateau.

Piezometers were placed in holes drilled with a hand auger at three observation sites, Obs1, Obs2, and Obs3, to form a transect perpendicular to the lake (Fig. 1b). The land surface slope and hydraulic gradient along the section were 1.7% and 1.0%, respectively. The depth of the piezometers varied between 2 and 4 m, depending on the DWT of the site. Each was constructed using a PVC pipe with a diameter of 50 mm, screened over the entire length of the subsurface. Augured sand was backfilled around the piezometers, and granular bentonite was then packed around the land surface to avoid preferential flow. The PVC pipes were capped to prevent direct rainfall and evaporation losses. The distance between Obs1 and Obs2 was approximately 300 m, while the distance between Obs2 and Obs3 was approximately 250 m. Obs1 and Obs2 were located in the low-lying area where the vadose zone consisted of fine to silty sand. In contrast, Obs3 was in the uplands, where both sand and sandstone lay within the unsaturated zone (Fig. 1b).

The hourly water table was monitored with a Keller DCX-22A data logger (Keller AG für Druckmesstechnik, Switzerland) that measured both the total pressure and barometric pressure, to account for the effect of barometric pressure. The barometric pressure transducers were positioned in a buffered thermal condition to exclude thermal effects (McLaughlin, 2011). A five-point moving average was used to smooth the groundwater level data (Loheide, 2008).

A rain gauge (Onset Computer, USA) was installed to monitor hourly rainfall approximately 400 m east of Obs3. Daily reference evapotranspiration (ET_0) was calculated using an ET_0 calculator (Food and Agriculture Organization of the United Nations, Italy). The required meteorological data (i.e., net radiation, air temperature, air humidity, and wind speed) were collected from the closest meteorological station.

The closest meteorological station is approximately 20 km southeast of the study area, but its monitoring data can represent the meteorological conditions of the study site because of its flat topography. Based on long-term data (2000–2017), the mean annual precipitation is 330 mm, with a significant annual variation indicated by a coefficient of variation (CV) of 0.3. Over 70% of the annual precipitation falls from June to September (Fig. 1c), and rainfall events with less than 5 mm are dominant, accounting for 72% of the total events (data not shown). The ET_0 calculated by the Penman-Monteith equation (Allen et al., 1998) is fairly stable at 1150 mm/a, with a CV as low as 0.1. The monthly ET_0 ranges from 22 mm in January to 203 mm in May, with an average value of 105 mm. The annual mean air temperature is approximately 7.0°C, with a maximum of 22.4°C in July and a minimum of –11.0°C in January (Fig. 1c).

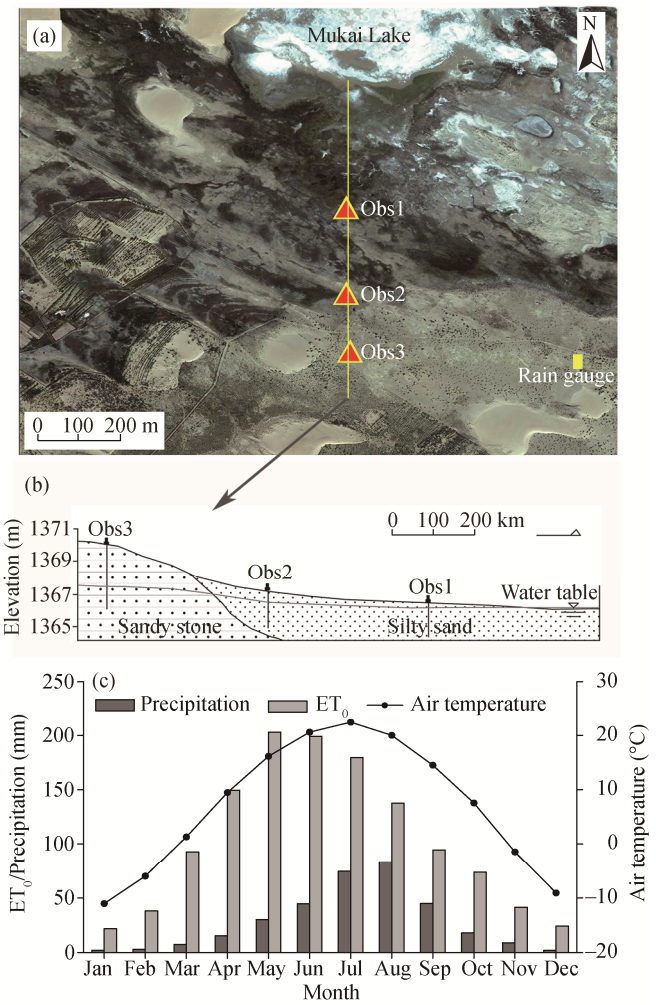

Fig. 1 (a) Location map showing the satellite image of the study sites (Obs1, Obs2 and Obs3); (b) the schematic hydrogeological cross section from measurements of the piezometers that are located at the bottom of wells; and (c) long-term average monthly precipitation, reference evapotranspiration (ET_0), and air temperature

2.2 Groundwater recharge estimation

The WTF method is widely applied for estimating the groundwater recharge of shallow unconfined aquifers, assuming that the rise of the water table in unconfined aquifers results solely from rainfall infiltration (Healy and Cook, 2002; Varni et al., 2013). The method is best applied in areas with shallow water tables that demonstrate sharp rises in the water table over short time periods. A previous study (Yin et al., 2011b) indicated that the WTF method is applicable to this study site. Groundwater recharge (R) is calculated as follows:

$$R=\frac{S_y dh}{dt}=\frac{S_y \Delta h}{\Delta t}, \tag{1}$$

where S_y is the specific yield; d is the DWT (cm); h is the hydraulic head (cm); t is the time (h); Δh is defined as the difference between the peak of the rise and the low point of the extrapolated antecedent recession curve at the time of the peak to determine the total recharge; and Δt is the time span corresponding to Δh.

2.3 ET_g estimation

Several methods are available for estimating ET_g based on diurnal WTFs, including those based on the water balance principle (White, 1932; Loheide, 2008) and those based on statistical theory

(Soylu et al., 2012; Wang and Pozdniakov, 2014). The method developed by Loheide (2008) was adopted here because of its capability to estimate hourly groundwater consumption, rather than daily values commonly obtained from other methods. A method comparison conducted previously also indicated that the Loheide method yielded the most accurate estimation (Yin et al., 2013). The Loheide method is based on three assumptions: (1) the decline in groundwater levels is only due to plant root water uptake and surface evaporation; (2) ET_g consumed by vegetation is negligible from midnight to 06:00; and (3) the rate of head change at the recovery source is equal to the overall rate of water table change at the observation location. The ET_g can be calculated using the groundwater balance equation:

$$\mathrm{ET_g}(t) = r(t) - S_y \times \frac{\Delta h}{\Delta t}, \tag{2}$$

where $r(t)$ is the net inflow rate of groundwater (mm/h); S_y is the specific yield of sediments; and $\Delta h/\Delta t$ is the change in DWT per unit time (mm/h). Because of the assumption that the rate of head change at the recovery source is equal to the overall rate of water table change at the observation location, the detrended water table depth (WT_{DT}) is obtained by subtracting this trend from a portion of the observed water table records as follows:

$$\mathrm{WT_{DT}}(t) = \mathrm{WT}(t) - m_T \times t - b_T, \tag{3}$$

where $WT(t)$ is the measured water table (mm); and m_T and b_T are the slope (mm/h) and intercept of the trend (mm), respectively. A relationship can be determined to predict $d\mathrm{WT_{DT}}/dt$ as a function, $\Gamma(\mathrm{WT_{DT}})$, of the detrended DWT using periods of zero ET_g. Subsequently, the net inflow rate of groundwater can be estimated using the following equation:

$$r(t) = S_y \times \left[\Gamma(\mathrm{WT_{DT}}(t)) + m_T\right]. \tag{4}$$

As the fastest recovery of the water table occurred around 21:00 (LST) at Obs1 and 00:00 at Obs2 (Fig. 2a), the groundwater inflow was calculated using the recovery period from 21:00 to 05:00 at Obs1 and 00:00 to 06:00 at Obs2, following the suggestion of Yin et al. (2013) that the fastest recovery of water table is an indicator of the suspension of ET_g.

2.4 Specific yield estimation

It should be noted that S_y is the most crucial factor in determining the accuracy of recharge and ET_g (Nachabe, 2002; Loheide et al., 2005; Gribovszki, 2017). S_y is defined as the volume of water released under gravity from storage per unit cross-sectional area, per unit decline in the water table (Freeze and Cherry, 1979). When the water table is deep (>1 m), the application of a constant S_y is valid (Duke, 1972; Soylu et al., 2012). However, depth-dependent S_y should be considered in shallow water table conditions (Crosbie et al., 2005; Loheide, et al., 2005; Fan et al., 2014; Cheng et al., 2017) . At Obs1 and Obs2, with shallow water tables, two methods were employed to estimate S_y. The relationship between S_y and DWT can be described by Equation 5.

$$S_y = \theta_s - \left[\theta_r + \frac{\theta_s - \theta_r}{(1 + (\alpha d)^n)^m}\right], \tag{5}$$

where d is the DWT (cm); θ_s is the saturated soil moisture (cm^3/cm^3); θ_r is the residual soil moisture (cm^3/cm^3); and α, n, and m are the empirical coefficients in the van Genuchten model (van Genuchten, 1980). Undisturbed soil samples were collected every 20 cm from the excavated profiles. Bulk density was estimated by the oven drying method, and particle-size distributions were determined by the sieving method for the sand fractions and by a soil hydrometer for the silt and clay fractions, respectively.

S_y was also determined by the water table response to rainfall events, as the ratio of infiltrated rainfall to recorded rise in water table level. Rainfall events were only considered when soil moisture was likely to be replenished by previous rainfall. The interception loss by the plant canopy was ignored because the grasses were small and sparsely distributed at the study sites. The S_y of sandstone at Obs3 was assumed to be constant because the water table was deeper than 3 m. We assigned the value of 0.08 to S_y based on a previous study (Yin et al., 2011b), which determined it through a pumping test that used the type-curve method.

3 Results and discussion

3.1 Variation of water table

The monitored DWT values at Obs1 and Obs2 from December 2017 to March 2018 were excluded because the soil was frozen. The patterns of water table variations were strongly related to DWT. At Obs1, Obs2, and Obs3, DWT varied between 0 and 70, 0 and 100, and 330 and 370 cm, respectively (Fig. 2a), with mean values of 20, 60, and 350 cm, respectively. Hourly groundwater levels at Obs1 responded to rainfall rapidly (usually within 1 h, data not shown), and levels were the highest among the three observation sites. The water table at Obs2 had similar but somewhat slower responses to rainfall (within 1–2 h) and was lower compared to that at Obs1. For example, the water table raised by 10 cm following a rainfall of 11.0 mm/d on 8 July 2017, at Obs2, while it rose by 27 cm at Obs1. The water table at Obs3 displayed a smooth and seasonal variation, and only reacted to heavy rainfall at the end of July and October, with a delay of approximately four days (Fig. 2a).

Diurnal fluctuations were observed for the entire observation period at Obs1, except during rainy periods (Fig. 2a). At Obs2, diurnal signals were obvious when the DWT was less than 75 cm, and diminished when the water table was lower, a behavior previously observed by others (Mould et al., 2010; Nippert et al., 2010). The diurnal magnitude was much higher at Obs1 than at Obs2, which had a deeper water table. For instance, the mean magnitude was 4.4 cm during 5–14 June 2018 at Obs1, three times higher than that at Obs2 (Fig. 2a). It was also observed that the water table began to decline approximately 2 h earlier at Obs1 than at Obs2 (Fig. 2b). In contrast, the water table at Obs3 did not show any diurnal fluctuations (Fig. 2a). The response to rainfall and the magnitude of diurnal fluctuations are attributed to the thickness of the unsaturated zones, which determines whether plants can extract groundwater.

The seasonal water table regime was controlled by meteorological conditions (rainfall and ET_0). In the study area, a hydrological year can be divided into a dry season (April–mid-July) and a wet season (the remaining period) (Yin et al., 2015). The DWT at Obs1 and Obs2 also reflected the characteristics of dry and wet seasons (Fig. 2c). In the dry season, the water table generally declined in response to lower rainfall and high ET_0, while in the wet season, the water table rose because of the increase in rainfall and decline in ET_0.

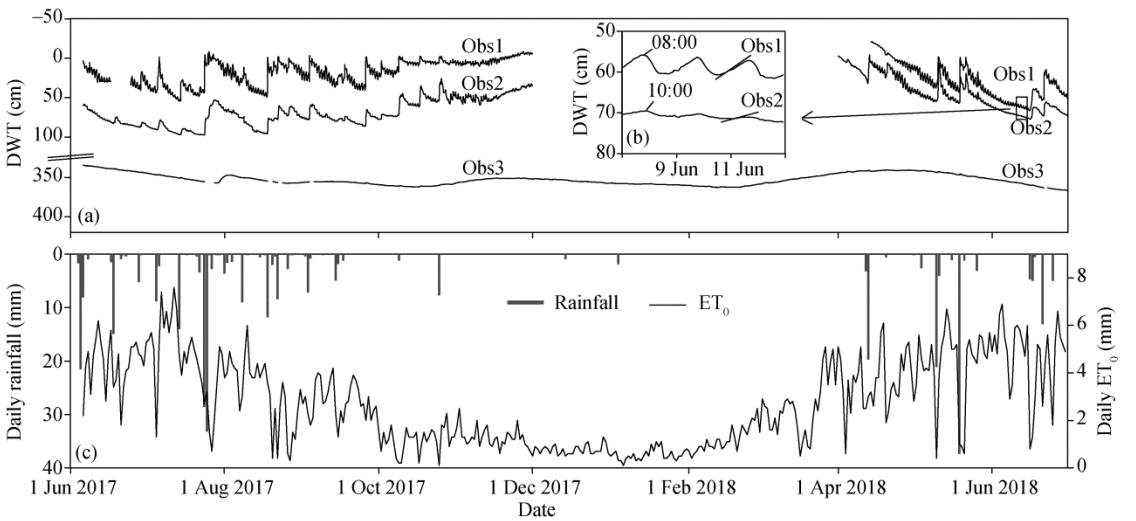

Fig. 2 Water table regimes at three observation sites, Obs1, Obs2, and Obs3 (a and b), daily rainfall and potential evapotranspiration (ET_0) (c). DWT, depth to water table.

3.2 Specific yield (S_y)

Soil texture analysis indicated that the soil was quite homogenous at Obs1 and Obs2; therefore, a uniform texture was assumed to estimate S_y using Equation 5. S_y estimated using the water table

response to rainfall and by soil texture, decreased with DWT (Fig. 3). The sample data and fitted exponential function (R^2=0.75, P<0.01) are shown in Figure 3. For silty sand soils, such as those at our sites, S_y was found to increase with DWT and also fitted an exponential pattern, reaching a relatively stable value within 1 m (Crosbie et al., 2005; Fan et al., 2014; Hill and Durchholz, 2015; Cheng et al., 2017). The relationship indicated that S_y varied significantly, with the difference of an order of magnitude in extreme cases, suggesting that ignoring S_y variations will result in substantial interpretation errors at sites with a shallow water table.

However, it should be noted that S_y from the water table response method was lower than that obtained using the soil texture method (Fig. 3). Differences have been widely observed among S_y obtained from commonly used methods, that is, soil texture, drainage, and water table response methods (Fan et al., 2014; Gribovszki, 2017). Method comparisons indicate that S_y values obtained using the water table response method are suitable for analyzing groundwater recharge, as the same temporal and spatial scales are used (Crosbie et al., 2005). Therefore, S_y from the water table response method was applied to estimate the groundwater recharge, whereas S_y from the soil texture method was used to calculate ET_g.

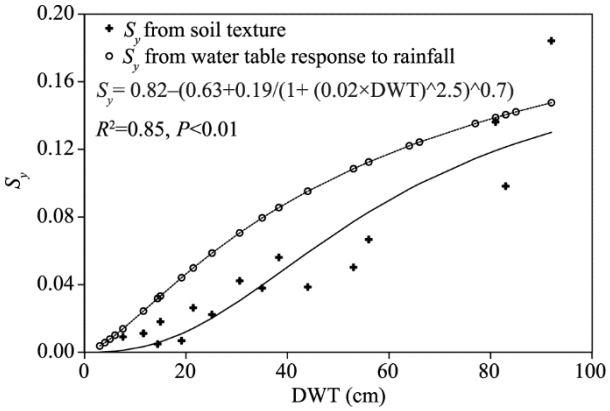

Fig. 3 Increases in specific yield (S_y) with DWT using the water table response method and the soil texture method

Soil water moisture before rainfall is a vital factor when using the water table response method to estimate S_y. Rainfall recharges soil water if the water content of the unsaturated zone is low, leading to an overestimation of S_y. Therefore, such rainfall events were only considered when soil moisture in the unsaturated zone was likely to be replenished by previous rainfall within one week of S_y estimation (Fan et al., 2014). However, this can also lead to significant errors when the water table is deeper, similarly to the S_y with DWT of 92 cm in Figure 3. In addition, intense rainfall can cause air from the unsaturated zone to infiltrate into the saturated zone, leading to a rapid rise in the water table. This process is called the Lisse effect (Crosbie et al., 2005; Miyazaki et al., 2012), which often causes the underestimation of S_y. However, in the study area, the Lisse effect was considered to be minimal, owing to the coastal soil texture.

3.3 Groundwater recharge

For Obs1 and Obs2, groundwater recharge was estimated for 26 rainfall events during June 2017 to June 2018. Groundwater recharge generally increased with the daily rainfall intensity (Fig. 4a). The rate of increase slowed when rainfall exceeded 20 mm/d and even decreased when rainfall was higher than 30 mm/d at Obs2. This phenomenon was attributed to heavy rainfall exceeding the infiltration capacity of soil (Horton, 1933; Beven, 2004; Liu et al., 2011), or to the elevation of the water table to the land surface, leaving no space for infiltration (Sophocleous, 2002; Hoang et al., 2017), with rainfall becoming surface runoff.

At the event scale, groundwater recharge was also affected by hourly rainfall intensity. For example, the rainfall amount was approximately 28.6 and 33.2 mm on 24 and 26 July 2017, respectively, however, the groundwater recharge on 26 July was much lower (13.4 mm) than that

on 24 July (23.9 mm) at Ob2 (Fig. 4b). Although rainfall was heavier on 26 July, it mostly fell within 1 h (approximately 21.7 mm/h). In comparison to the prolonged rainfall on 24 July, the concentrated rainfall reduced groundwater recharge, as rainfall mainly became surface runoff. The relationship between rainfall intensity and groundwater recharge indicates that groundwater resources will decrease under the projected climate change, in which heavy rainfall events will increase with an overall reduction in rainfall frequency (Allen and Ingram, 2002).

Antecedent rainfall also affected groundwater recharge in some cases. For instance, groundwater recharge was approximately 6.9 mm/d when the rainfall amount was 14.9 mm on 18 June 2017, while it reached 12.8 mm on 21 June 2018 when the rainfall was slightly lower (13.1 mm/d). It was found that the five-day cumulative rainfall was 1.5 mm for the first case and much lower than 10.2 mm for the latter event. The antecedent rainfall increased soil moisture, and subsequent rainfall replenished soil moisture and produced more recharge than the case in which the soil was dry and most infiltrated rainfall was retained in vadose zones (Zhang and Schilling, 2006).

In addition, groundwater was also determined by DWT as groundwater recharge at Obs2 was higher than that at Obs1, with a shallower water table in most cases (Fig. 4a). However, the relationship between groundwater recharge and DWT was nonlinear. For example, the total groundwater recharge during the study period was the highest at Obs2, corresponding to a mean DWT of 72 cm in the rainy period, compared to that at the shallowest site (mean DWT, 30 cm at Obs1) or at the deepest site (mean DWT, 360 cm at Obs3). It seems that both deeper and shallower water tables restrict groundwater recharge. In areas where the water table is close to the land surface, such as Obs1, rainfall mainly becomes surface runoff due to the saturation of the ground, instead of infiltration to groundwater (Gillham, 1984). At sites with thick unsaturated zones, such as Obs3, the majority of rainfall infiltration is consumed by evapotranspiration in the uppermost 2 m of soil in semi-arid regions (Cook et al., 1989), and only a small portion reaches groundwater.

At the monthly scale, the temporal variations of groundwater recharge at Obs1 and Obs2 were similar and generally determined by the amount of rainfall (Fig. 4c). The greatest recharge

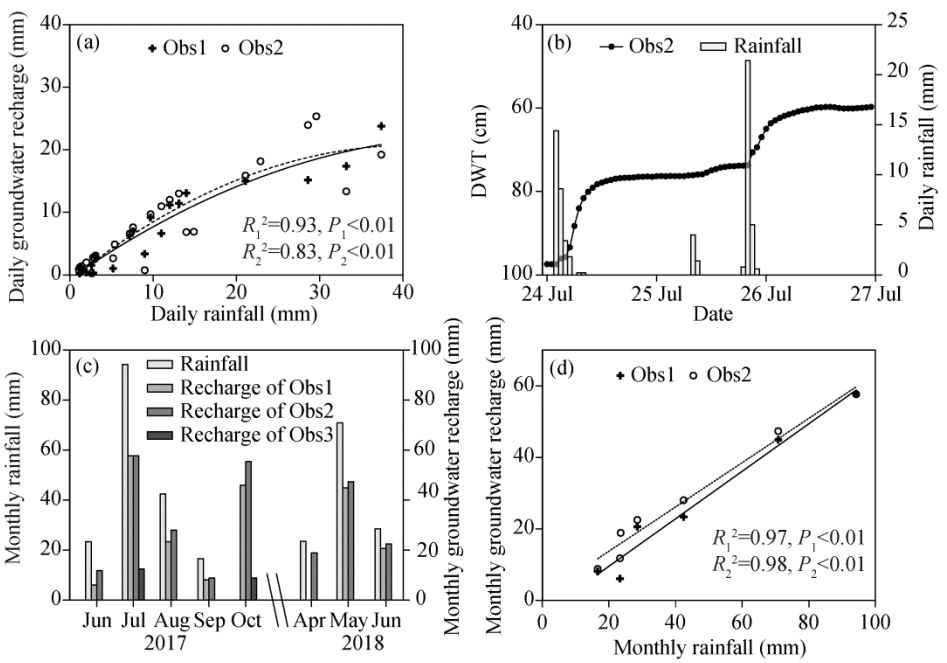

Fig. 4 Relationships between event-based groundwater recharge and rainfalls at Obs1 and Obs2 (a), water table fluctuations in response to rainfall at 00:00 on 24 and 26 July 2017 (b), monthly groundwater recharge and rainfall (c), and their fitted relationships (d)

occurred in July 2017, corresponding to the heaviest monthly rainfall of 94.2 mm, while the lowest recharge occurred in September 2017, when the monthly rainfall was as low as 16.6 mm. A linear equation with a positive slope can be used to describe the relationship between the monthly groundwater recharge and rainfall (Fig. 4d). Groundwater recharge was usually higher at Obs2 at a monthly scale than that at Obs1 (Fig. 4c), as the mean DWT for Obs1 and Obs2 was 21.0 and 61.0 cm, respectively. During the study period, total groundwater recharge was approximately 207.0 mm, accounting for 52% of the rainfall at Obs1, while groundwater recharge was approximately 250.0 and 21.0 mm at Obs2 and Obs3, respectively, accounting for 63% and 5% of rainfall, respectively.

Overall, the recharge rate of Obs2 was higher than those of Obs1 and Obs3, indicating that both shallower and deeper water tables can limit rainfall recharge. The soil texture of the unsaturated zone in Obs3 was also a major factor that decreased the recharge rate. Compared with Obs1 and Obs2, similar recharge rates (53% and 62%) were also found in the study by Crosbie et al. (2005) and Fan et al. (2014) with similar soil textures and plants. Although the mean DWT (120.0 and 200.0 cm) of their study areas was greater, the annual rainfall was almost four times higher than that at our study site. Therefore, a greater DWT does not decrease the rainfall infiltration in case of a high water content in the unsaturated zones.

3.4 Groundwater evapotranspiration

As no diurnal fluctuations were observed at Obs3 (Fig. 2a), hourly ET_g (excluding rainy days), was estimated for Obs1 and Obs2 only. The period from November 2017 to March 2018 was excluded because the ET_g values were negligible due to plant dormancy (Yin et al., 2014). Therefore, ET_g was calculated for 129 d for Obs1 and 133 d for Obs2. It was observed that ET_g clearly varied diurnally. The mean ET_g for each hour shows that ET_g usually started increasing from 06:00 to a maximum of approximately 0.54 mm/h at 13:00 to 14:00, then decreased back to zero at 21:00 at Obs1 (Fig. 5). From 22:00 to 05:00 the next day, ET_g was close to zero, indicating that there was no groundwater uptake during the night. Hourly ET_g variations at Obs2 were similar to those at Obs1 (R^2=0.91, P<0.01), except that the peak values were lower (approximately 0.29 mm/h) and the duration of the peak was longer (approximately 4 h versus 2 h at Obs1) (Fig. 5). During daytime, the standard deviation (SD) of ET_g increased with time, reaching a peak value at 13:00, and then decreased. For example, SD increased from 0.05 mm/h at 06:00 to 0.27 mm/h at 13:00, and decreased nearly to 0.00 mm/h at 21:00 at Obs1.

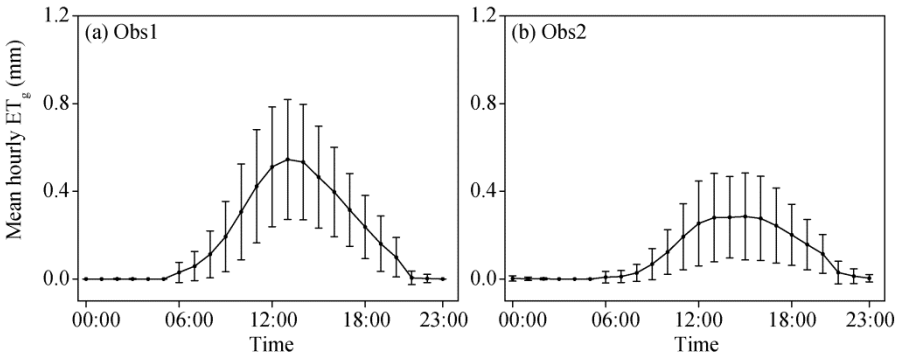

Fig. 5 Mean hourly ET_g (groundwater evapotranspiration) at Obs1 (a) and Obs2 (b)

Daily ET_g patterns suggested that it started to increase around mid-April when plants began to grow and became nearly zero in mid-October when they entered winter dormancy (Fig. 6), with good agreement on daily sap flow variations in the Mu Us Sandy Land of China (Yin et al., 2014). At a daily scale, ET_g at Obs1 ranged from 0.3 to 8.7 mm/d, with a mean value of 4.3 mm/d, while at Obs2 it varied between 0.1 and 7.8 mm/d, with a mean value of 2.5 mm/d. It should be noted that ET_g at Obs1 and Obs2 was in line with other grass-covered areas, where it is reported to be in the range of 1.0–4.0 mm/d (Nachabe et al., 2005; Schilling, 2007; Lautz, 2008; Gribovszki et al.,

2017). Meteorological conditions were the main factors affecting the fluctuations in daily ET_g. The correlation analysis revealed that net radiation and vapor pressure deficit and relative humidity were positively and negatively related to ET_g, respectively (Fig. 7a, b and c). However, there was no correlation between ET_g and wind speed (Fig. 7d). The most influential meteorological factors on ET_g were net radiation, relative humidity, vapor pressure deficit, and wind speed.

Although hourly and daily ET_g at Obs1 and Obs2 exhibited similar temporal variations, the magnitudes were substantially different (Figs. 5 and 6). It was hypothesized that DWT, the main difference between the two sites, caused this difference. To explore the impact of DWT on ET_g, we introduced the ratio of ET_g to ET_0, as meteorological conditions also affect ET_g in shallow water table conditions, as shown in Figure 7 and other studies (Butler et al., 2007; Carlson Mazur et al., 2014; Shanafield et al., 2017). ET_g/ET_0 gradually decreased with DWT and an exponential equation was used to fit this decay (Fig. 8a), which is consistent with field observations (Nichols, 1994; Cooper et al., 2006; Elmore et al., 2006; Pritchett and Manning, 2012; Ma et al., 2013; Shen et al., 2015; Liu et al., 2017) and numerical modeling (Shah et al., 2007; Soylu et al., 2012). It is predicted that, based on an extrapolation using the fitted equation, ET_g/ET_0 will drop to 0.005

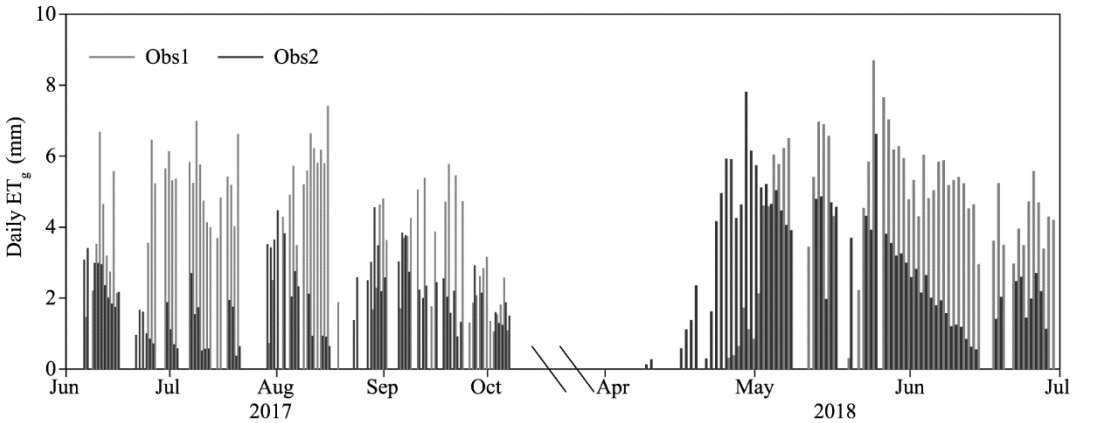

Fig. 6 Daily ET_g at Obs1 and Obs2

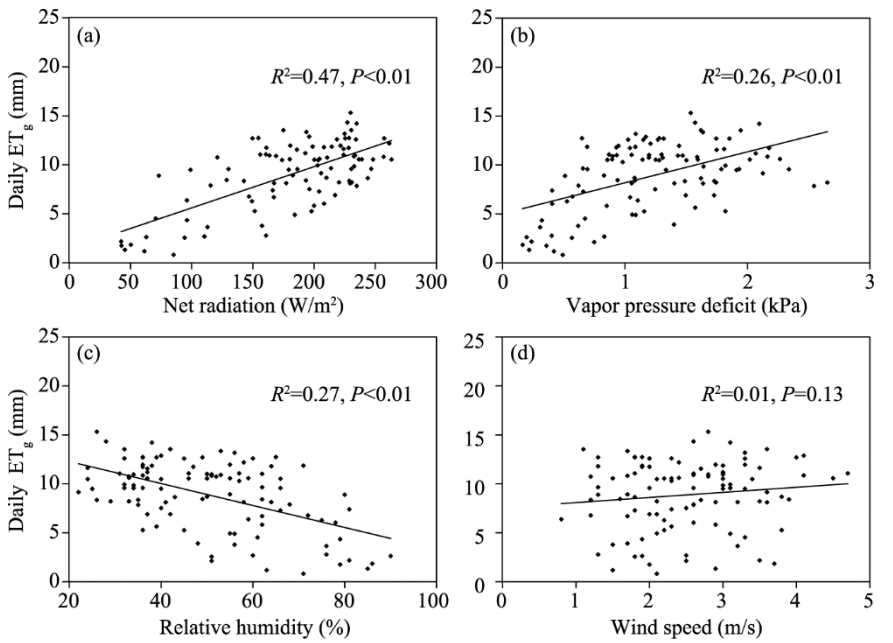

Fig. 7 Relationships of daily ET_g with net radiation (a), vapor pressure deficit (b), relative humidity (c), and wind speed (d)

when the water table decreases to 3.0 m. The depth corresponding to an ET_g/ET_0 value below 0.005 is defined as the extinction depth (Shah et al., 2007), which is a key parameter for quantifying regional evapotranspiration. The extinction depth of the study site was approximately 3.0 m, explained by the absence of diurnal fluctuations at Obs3, where the mean DWT was approximately 3.5 m.

The monthly ET_g was obtained by summing daily values. On a monthly scale, ET_g ranged from 125.0 mm in June 2018 to 4.0 mm in April 2018, with a mean value of 67.0 mm at Obs1, while ET_g ranged from 94.0 mm in May 2018 to 8 mm in October 2017, with a mean value of 42.0 mm at Obs2. The coefficient of determination (R^2) between ET_g and ET_0 at Obs1 was 0.94, which was higher than that at Obs2 (R^2=0.29), indicating that ET_g at Obs1 was mainly determined by meteorological conditions. ET_g at Obs2 was also controlled by DWT, as indicated by the lower values in July 2017 and June 2018, when the water table was at its lowest (Figs. 2a and 8b), although ET_0 in those times was higher than that during the neighboring months (Fig. 8b). The monthly variations in ET_g suggested that ET_g was determined by the DWT and meteorological conditions.

Over the hydrological year studied, the groundwater consumption at Obs1 was approximately 539.0 mm, which was 1.6 times the annual rainfall. At Obs2 it was approximately 336.0 mm, equivalent to 0.9 times the annual rainfall, indicating strong groundwater uptake by ET_g in shallow water table areas. In shallow water table environments, ET_g can significantly exceed rainfall, as shown in this and previous studies. For example, in a playa in arid central Australia, annual ET_g loss is as high as annual rainfall (Shanafield et al., 2015). In the riparian zones of the Middle Rio Grande River, the estimated ET_g is even higher, approximately four times the annual rainfall (Soylu et al., 2012).

Additionally, the variation patterns of rainfall recharge and ET_g were only analyzed for one hydrological year because of limited monitoring data. In the future, the interannual variations of rainfall recharge and ET_g and their determining factors should be explored.

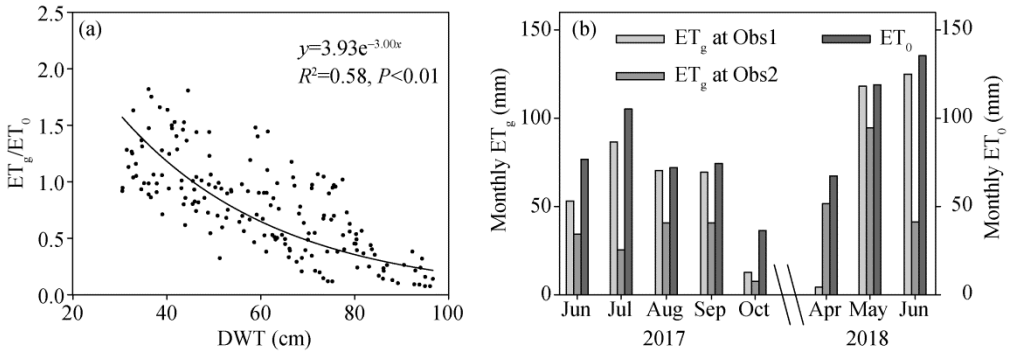

Fig. 8 Relationship between DWT and ET_g/ET_0 (a) and monthly ET_0 and ET_g variations at Obs1 and Obs2 (b)

4 Conclusions

In this study, WTFs in three observation wells along a cross-sectional area were observed over a hydrological year, in a semi-arid lake wetland in the Ordos Plateau, China. The data were analyzed to estimate groundwater recharge and evapotranspiration using a depth-dependent specific yield. A rapid water table response to rainfall was observed for two shallow wells (i.e., Obs1 and Obs2), at which diurnal WTFs were also observed over most of the study period. This indicated that the most influential factors of variations in water table level are rainfall and ET_g. However, at the deeper water table site (Obs3), the groundwater table only reacted to extremely heavy rainfall and showed no diurnal variations.

Over the study period, the annual groundwater recharge was 207.0, 250.0, and 21.0 mm, accounting for 52%, 63%, and 5% of rainfall at Obs1, Obs2, and Obs3, respectively. It was found that rainfall intensity is one of the main determining factors for rainfall infiltration, as

groundwater recharge increases with rainfall intensity at daily and monthly scales, and the rate of increase of daily groundwater recharge slowed down when rainfall exceeded 20–30 mm/d, due to surface runoff. In addition, DWT was also a major factor influencing groundwater recharge, according to the recharge rate of the three observation wells in this study.

Hourly ET_g showed that groundwater consumption occurred mainly during the daytime, and nighttime ET_g was negligible. The daily mean ET_g at Obs1 and Obs2 were 4.3 and 2.5 mm, respectively, over the entire hydrological year. The variations in ET_g were mainly attributed to the DWT and net radiation in the study area.

Acknowledgements

This research was funded by the National Natural Science Foundation of China (41472228, 41877199) and the Key Laboratory of Groundwater and Ecology in Arid Regions of China Geological Survey and Innovation Capability Support Program of Shaanxi Province, China (2019TD-040). The authors would like to express their thanks to Dr. Neville ROBINSON for polishing the language.

References

Allen M R, Ingram W J. 2002. Constraints on future changes in climate and the hydrologic cycle. Nature, 419(6903): 224–232.

Allen R G, Pereira L S, Raes D, et al. 1998. Crop Evapotranspiration-Guidelines for Computing Crop Water Requirements. FAO Irrigation and Drainage Paper 56, Rome, Italy.

Alley W M, Healy R W, LaBaugh J W, et al. 2002. Flow and storage in groundwater systems. Science, 296(5575): 1985–1990.

Allison G B, Gee G W, Tyler S W. 1994. Vadose-zone techniques for estimating groundwater recharge in arid and semiarid regions. Soil Science Society of America Journal, 58(1): 6–14.

Baird K J, Maddock I T. 2005. Simulating riparian evapotranspiration: a new methodology and application for groundwater models. Journal of Hydrology, 312(1–4): 176–190.

Beven K. 2004. Infiltration excess at the Horton Hydrology Laboratory (or not?). Journal of Hydrology, 293(1–4): 219–234.

Bredehoeft J. 1997. Safe yield and the water budget myth. Groundwater, 35(6): 929.

Busch D E, Ingraham N L, Smith S D. 1992. Water uptake in woody riparian phreatophytes of the southwestern United States: a stable isotope study. Ecological Applications, 2(3): 450–459.

Butler J J, Kluitenberg G J, Whittemore D O, et al. 2007. A field investigation of phreatophyte-induced fluctuations in the water table. Water Resources Research, 43(2): 299–309.

Carlson Mazur M L, Wiley M J, Wilcox D A. 2014. Estimating evapotranspiration and groundwater flow from water-table fluctuations for a general wetland scenario. Ecohydrology, 7(2): 378–390.

Chang X C, Wang M Z, Han Z Z. 2006. Coexistence and inherence of diverse energy resources in the Ordos Basin, China. Chinese Journal of Geochemistry, 25(4): 386–390.

Cheng D, Duan J, Qian K, et al. 2017. Groundwater evapotranspiration under psammophilous vegetation covers in the Mu Us Sandy Land, northern China. Journal of Arid Land, 9(1): 98–108.

Cook P G, Walker G R, Jolly I D. 1989. Spatial variability of groundwater recharge in a semiarid region. Journal of Hydrology, 111(1–4): 195–212.

Cooper D J, Sanderson J S, Stannard D I, et al. 2006. Effects of long-term water table drawdown on evapotranspiration and vegetation in an arid region phreatophyte community. Journal of Hydrology, 325(1–4): 21–34.

Crosbie R S, Binning P, Kalma J D. 2005. A time series approach to inferring groundwater recharge using the water table fluctuation method. Water Resources Research, 41(1): W01008, doi: 10.1029/2004WR003077.

Dai S, Ren D, Chou C L, et al. 2006. Mineralogy and geochemistry of the No. 6 coal (Pennsylvanian) in the Junger Coalfield, Ordos Basin, China. International Journal of Coal Geology, 66(4): 253–270.

Delottier H, Pryet A, Lemieux J M, et al. 2018. Estimating groundwater recharge uncertainty from joint application of an aquifer test and the water-table fluctuation method. Hydrogeology Journal, 26(7): 2495–2505.

Diouf O C, Weihermüller L, Diedhiou M, et al. 2020. Modelling groundwater evapotranspiration in a shallow aquifer in a semi-arid environment. Journal of Hydrology, 587: 124967, doi: 10.1016/j.jhydrol.2020.124967.

Doble R C, Crosbie R S. 2017. Current and emerging methods for catchment-scale modelling of recharge and evapotranspiration from shallow groundwater. Hydrogeology Journal, 25(1): 3–23.

Doll P, Schmied H M, Schuh C, et al. 2014. Global-scale assessment of groundwater depletion and related groundwater

abstractions: Combining hydrological modeling with information from well observations and GRACE satellites. Water Resources Research, 50(7): 5698–5720.

Duke H R. 1972. Capillary properties of soils-influence upon specific yield. Transactions of the ASAE, 15(4): 688–691.

Elmore A J, Manning S J, Mustard J F, et al. 2006. Decline in alkali meadow vegetation cover in California: the effects of groundwater extraction and drought. Journal of Applied Ecology, 43(4): 770–779.

Fan J, Oestergaard, K T, Guyot A, et al. 2014. Estimating groundwater recharge and evapotranspiration from water table fluctuations under three vegetation covers in a coastal sandy aquifer of subtropical Australia. Journal of Hydrology, 519: 1120–1129.

Fan Y, Li H, Miguez-Macho G. 2013. Global patterns of groundwater table depth. Science, 339(6122): 940–943.

Feng W, Zhong M, Lemoine J M, et al. 2013. Evaluation of groundwater depletion in North China using the Gravity Recovery and Climate Experiment (GRACE) data and ground-based measurements. Water Resources Research, 49(4): 2110–2118.

Freeze R A, Cherry J A. 1979. Ground Water. Prentice Hall, Englewood Cliffs, 604.

Gillham R W. 1984. The capillary fringe and its effect on water-table response. Journal of Hydrology, 67(1–4): 307–324.

Gribovszki Z, Kalicz P, Szilágyi J, et al. 2008. Riparian zone evapotranspiration estimation from diurnal groundwater level fluctuations. Journal of Hydrology, 349(1–2): 6–17.

Gribovszki Z, Szilágyi J, Kalicz P. 2010. Diurnal fluctuations in shallow groundwater levels and streamflow rates and their interpretation–A review. Journal of Hydrology, 385(1–4): 371–383.

Gribovszki Z. 2017. Comparison of specific-yield estimates for calculating evapotranspiration from diurnal groundwater-level fluctuations. Hydrogeology Journal, 26(3): 869–880.

Gribovszki Z, Kalicz P, Balog K, et al. 2017. Groundwater uptake of different surface cover and its consequences in great Hungarian plain. Ecological Processes, 6(1): 39.

Gribovszki Z. 2018. Validation of diurnal soil moisture dynamic-based evapotranspiration estimation methods. Quarterly Journal of the Hungarian Meteorological Service, 122(1): 15–30.

Healy R W, Cook P G. 2002. Using groundwater levels to estimate recharge. Hydrogeology Journal, 10(1): 91–109.

Hill A J, Durchholz B. 2015. Specific yield functions for estimating evapotranspiration from diurnal surface water cycles. Journal of the American Water Resources Association, 51(1): 123–132.

Hoang L, Schneiderman E M, Moore K E B, et al. 2017. Predicting saturation-excess runoff distribution with a lumped hillslope model: SWAT-HS. Hydrological Processes, 31(12): 2226–2243.

Horton R E. 1933. The role of infiltration in the hydrologic cycle. Eos, Transactions American Geophysical Union, 14(1): 446–460.

Hou G C, Liang Y P, Su X S, et al. 2008. Groundwater systems and resources in the Ordos Basin, China. Acta Geologica Sinica (English Edition), 82(5): 1061–1069.

Lautz L K. 2008. Estimating groundwater evapotranspiration rates using diurnal water-table fluctuations in a semi-arid riparian zone. Hydrogeology Journal, 16(3): 483–497.

Liu B, Guan H, Zhao W, et al. 2017. Groundwater facilitated water-use efficiency along a gradient of groundwater depth in arid northwestern China. Agricultural and Forest Meteorology, 233: 235–241.

Liu F, Song X, Yang L, et al. 2015. The role of anthropogenic and natural factors in shaping the geochemical evolution of groundwater in the Subei Lake basin, Ordos energy base, Northwestern China. Science of the Total Environment, 538: 327–340.

Liu F, Song X, Yang L, et al. 2018. Predicting the impact of heavy groundwater pumping on groundwater and ecological environment in the Subei Lake basin, Ordos energy base, Northwestern China. Hydrology Research, 49(4): 1156–1171.

Liu H, Lei T W, Zhao J, et al. 2011. Effects of rainfall intensity and antecedent soil water content on soil infiltrability under rainfall conditions using the run off-on-out method. Journal of Hydrology, 396(1–2): 24–32.

Liu Y, Yamanaka T, Zhou X, et al. 2014. Combined use of tracer approach and numerical simulation to estimate groundwater recharge in an alluvial aquifer system: A case study of Nasunogahara area, central Japan. Journal of Hydrology, 519: 833–847.

Loheide S P, Butler J J, Gorelick S M. 2005. Estimation of groundwater consumption by phreatophytes using diurnal water table fluctuations: A saturated-unsaturated flow assessment. Water Resources Research, 41(7): 1–14.

Loheide S P. 2008. A method for estimating subdaily evapotranspiration of shallow groundwater using diurnal water table fluctuations. Ecohydrology, 1(1): 59–66.

Ma J, Huang X, Li W, et al. 2013. Sap flow and trunk maximum daily shrinkage (MDS) measurements for diagnosing water status of Populus euphratica in an inland river basin of Northwest China. Ecohydrology, 6(6): 994–1000.

McLaughlin D L, Cohen M J. 2011. Thermal artifacts in measurements of fine-scale water level variation. Water Resources Research, 47(9), doi: 10.1029/2010WR010288.

Meinzer O E. 1923. The occurrence of ground water in the United States with a discussion of principles. In: Geological Survey Water Supply Paper 489. US Government Printing Office.

Miyazaki T, Ibrahimi M K, Nishimura T. 2012. Shallow groundwater dynamics controlled by Lisse and reverse Wieringermeer effects. Journal of Sustainable Watershed Science and Management, 1(2): 36–45.

Mould D J, Frahm E, Salzmann T, et al. 2010. Evaluating the use of diurnal groundwater fluctuations for estimating evapotranspiration in wetland environments: case studies in southeast England and northeast Germany. Ecohydrology, 3(3): 294–305.

Nachabe M, Shah N, Ross M, et al. 2005. Evapotranspiration of two vegetation covers in a shallow water table environment. Soil Science Society of America Journal, 69(2): 492–499.

Nachabe M H. 2002. Analytical expressions for transient specific yield and shallow water table drainage. Water Resources Research, 38(10): 1193, doi: 10.1029/2001WR001071.

Nichols W D. 1994. Groundwater discharge by phreatophyte shrubs in the Great Basin as related to depth to groundwater. Water Resources Research, 30(12): 3265–3274.

Nippert J B, Butler Jr J J, Kluitenberg G J, et al. 2010. Patterns of *Tamarix* water use during a record drought. Oecologia, 162(2): 283–292.

Pritchett D, Manning S J. 2012. Response of an intermountain groundwater-dependent ecosystem to water table drawdown. Western North American Naturalist, 72(1): 48–59.

Sargeant C I, Singer M B. 2016. Sub-annual variability in historical water source use by Mediterranean riparian trees. Ecohydrology, 9(7): 1328–1345.

Scanlon B R, Faunt C C, Longuevergne L, et al. 2012. Groundwater depletion and sustainability of irrigation in the US High Plains and Central Valley. Proceedings of the National Academy of Sciences of the United States of America, 109(24): 9320–9325.

Schilling K E. 2007. Water table fluctuations under three riparian land covers, Iowa (USA). Hydrological Processes, 21(18): 2415–2424.

Scott M L, Lines G C, Auble G T. 2000. Channel incision and patterns of cottonwood stress and mortality along the Mojave River, California. Journal of Arid Environments, 44(4): 399–414.

Shah N, Nachabe M, Ross M. 2007. Extinction depth and evapotranspiration from ground water under selected land covers. Ground Water, 45(3): 329–338.

Shanafield M, Cook P G, Gutiérrez-Jurado H A, et al. 2015. Field comparison of methods for estimating groundwater discharge by evaporation and evapotranspiration in an arid-zone playa. Journal of Hydrology, 527: 1073–1083.

Shanafield M, Gutiérrez-Jurado H, Rodríguez-Burgueño J E, et al. 2017. Short-and long-term evapotranspiration rates at ecological restoration sites along a large river receiving rare flow events. Hydrological Processes, 31(24): 4328–4337.

Shen Q, Gao G, Fu B, et al. 2015. Responses of shelterbelt stand transpiration to drought and groundwater variations in an arid inland river basin of Northwest China. Journal of Hydrology, 531: 738–748.

Siebert S, Burke J, Faures J M, et al. 2010. Groundwater use for irrigation - a global inventory. Hydrology and Earth System Sciences, 14(10): 1863–1880.

Sophocleous M. 2002. Interactions between groundwater and surface water: the state of the science. Hydrogeology Journal, 10(1): 52–67.

Soylu M E, Lenters J D, Istanbulluoglu E, et al. 2012. On evapotranspiration and shallow groundwater fluctuations: A Fourier-based improvement to the White method. Water Resources Research, 48(6): W06506, doi: 10.1029/2011WR010964.

Toth J. 1962. A theory of groundwater motion in small drainage basins in central Alberta, Canada. Journal of Geophysical Research, 67(11): 4375–4388.

van Genuchten M T. 1980. A closed-form equation for predicting the hydraulic conductivity of unsaturated soils. Soil Science Society of America Journal, 44(5): 892–898.

Varni M, Comas R, Weinzettel P, et al. 2013. Application of the water table fluctuation method to characterize groundwater recharge in the Pampa plain, Argentina. Hydrological Sciences Journal, 58(7): 1445–1455.

Wang P, Pozdniakov S P. 2014. A statistical approach to estimating evapotranspiration from diurnal groundwater level fluctuations. Water Resources Research, 50(3): 2276–2292.

Wang T, Yu J, Wang P, et al. 2019a. Estimating groundwater evapotranspiration by phreatophytes using combined water level and soil moisture observations. Ecohydrology, 12(5): e2092, doi: 10.1002/eco.2092.

Wang T, Wang P, Yu J, et al. 2019b. Revisiting the White method for estimating groundwater evapotranspiration: a consideration of sunset and sunrise timings. Environmental Earth Sciences, 78(14): 412.

Wang W, Yang G, Wang G. 2010. Groundwater numerical model of Haolebaoji well field and evaluation of the environmental

problems caused by exploitation. South-to-North Water Transfers and Water Science and Technology, 8(6): 36–41.

White W N. 1932. A Method of Estimating Ground-water Supplies based on Discharge by Plants and Evaporation from Soil: Results of Investigations in Escalante Valley. In: Geological Survey Water Supply Paper 659-A. US Government Printing Office.

Yin L, Hou G, Dou Y, et al. 2011a. Hydrogeochemical and isotopic study of groundwater in the Habor Lake Basin of the Ordos Plateau, NW China. Environmental Earth Sciences, 64(6): 1575–1584.

Yin L, Hu G, Huang J, et al. 2011b. Groundwater-recharge estimation in the Ordos Plateau, China: comparison of methods. Hydrogeology Journal, 19(8): 1563–1575.

Yin L, Zhou Y, Ge S, et al. 2013. Comparison and modification of methods for estimating evapotranspiration using diurnal groundwater level fluctuations in arid and semiarid regions. Journal of Hydrology, 496: 9–16.

Yin L, Zhou Y, Huang J, et al. 2014. Dynamics of willow tree (*Salix matsudana*) water use and its response to environmental factors in the semi-arid hailiutu river catchment, northwest China. Environmental Earth Sciences, 71(12): 4997–5006.

Yin L, Zhou Y, Huang J, et al. 2015. Interaction between groundwater and trees in an arid site: Potential impacts of climate variation and groundwater abstraction on trees. Journal of Hydrology, 528: 435–448.

Zhang P, Yuan G, Shao M, et al. 2016. Performance of the White method for estimating groundwater evapotranspiration under conditions of deep and fluctuating groundwater. Hydrological Processes, 30(1): 106–118.

Zhang Y K, Schilling K E. 2006. Effects of land cover on water table, soil moisture, evapotranspiration, and groundwater recharge: a field observation and analysis. Journal of Hydrology, 319(1–4): 328–338.

Zhou Y. 2009. A critical review of groundwater budget myth, safe yield and sustainability. Journal of Hydrology, 370(1–4): 207–213.